COBEM 2021 26th International Congress of Mechanical Engineering
November 22-26, 2021, Virtual Congress, Brazil
ABCM Associação Brasileira de Engenharia e Ciências Mecânicas

COBEM2021-0567
NUMERICAL INVESTIGATION OF METASTABLE CONDENSATION OF WET STEAM UNDER HIGH-PRESSURE CONDITIONS

Luccas K. Kavabata
Department of Mechanical Engineering, University of São Paulo, Av. Professor Mello Moraes, 2231 - Butantã, São Paulo - SP, 05508-030, Brazil
luccas.kavabata@usp.br
Ulisses A. Costa
Department of Mechanical Engineering, University of São Paulo, Av. Professor Mello Moraes, 2231 - Butantã, São Paulo - SP, 05508-030, Brazil
ulisses.costa@usp.br
Arthur S. Cato
Department of Mechanical Engineering, University of São Paulo, Av. Professor Mello Moraes, 2231 - Butantã, São Paulo - SP, 05508-030, Brazil
arthur.cato@gmail.com
Jairo P. C. Filho
Department of Mechanical Engineering, University of São Paulo, Av. Professor Mello Moraes, 2231 - Butantã, São Paulo - SP, 05508-030, Brazil
jairo.paes@usp.br
João V. N. Nunes
Instituto de Aeronáutica e Espaço, DCTA/IAE, 12228-904, São José dos Campos, SP, Brazil
jvnfonseca@gmail.com
Ernani V. Volpe
Department of Mechanical Engineering, University of São Paulo, Av. Professor Mello Moraes, 2231 - Butantã, São Paulo - SP, 05508-030, Brazil
ernvolpe@usp.br
João L. F. Azevedo
Instituto de Aeronáutica e Espaço, DCTA/IAE, 12228-904, São José dos Campos, SP, Brazil
joaoluiz.azevedo@gmail.com
Marcelo T. Hayashi
Department of Aerospace Engineering, Federal University of ABC, Av. dos Estados, 5001 - Bangú, Santo André - SP, 09210-580, Brazil
mthayashi@gmail.com

Abstract. *Phase change involves complex phenomena and may occur in many engineering applications, such as compressors, low-pressure turbines and supersonic separators. In many of them, phase change is undesirable, since it may cause efficiency loss and service life reduction. However, there are applications where it is essential. Such is the case with the supersonic separator, where phase change is what allows the separation to occur. In fact, the device is designed to condense components of a gaseous mixture, so as to collect them. It accelerates that mixture to a supersonic flow in an isentropic expansion process, which entails the homogeneous meta-stable condensation of some components. Hence,it is of practical importance to investigate and control such phenomena. The task involves modeling nucleation and growth rates for the liquid (dispersed) phase, as well as deriving the equations that govern the evolution of liquid droplets in the gas flow. An attractive approach to that end is the so-called method of moments, which has been the focus of much research activity in recent years. The objective of the present work is to perform a numerical investigation of meta-stable condensing flows, for non-ideal single component gases under high-pressure conditions. The study is addressing the comparison of some well-known nucleation rate and growth rate models that are available in the literature for the problem.*

Keywords: *High pressure condensation, metastability, non-ideal compressible fluid dynamics, non-ideal equations of state*

1. INTRODUCTION

Phase change is a complex phenomena that may occur in many engineering applications, such as compressors, Low-Pressure turbines (LP turbines) supersonic separators, etc. In some cases, e.g., compressors, they are undesirable since

they may result in efficiency loss and a reduction of the service life of the device components, as is the case of LP turbines. In other cases, e.g., supersonic separators, they are essential. Therefore it is of practical importance to study such phenomena to either prevent or ensure that they occur, in order to design efficient engineering devices. Such studies require knowledge of the different circumstances under which phase change phenomena may occur, i.e., in equilibrium or non-equilibrium conditions, as well as the mechanism involved, i.e., homogeneous and/or heterogeneous nucleation. In addition, the investigations regarding phase change phenomena involve modeling the problem properly in order to perform suitable numerical simulations. The modeling for such cases requires the evaluation of the rate at which a new phase is formed, namely the nucleation rate, and the rate at which this new phase grows, the growth rate. Furthermore, it is necessary to evaluate the evolution of the new phase. One possibility is the so-called method of moments, which has been employed recently to investigate the evolution of the liquid phase in condensing gas/gas mixture flows.

The operation conditions for the different engineering applications may vary from low- to high- pressures. Such conditions are important since they are related to the complexity of the models employed. For low pressures, for instance, a few simplifying hypotheses may be made, such as to consider the vapor phase as an ideal gas. These hypotheses greatly simplify the models and calculations. On the other hand, if the device is subjected to high pressures, then the compressibility factor (z) may be quite different from unity, meaning that the ideal gas hypothesis can no longer be assumed. Hence, for such cases, equations of state (EoS) capable of accurately predicting non-ideal gas behavior are necessary. Such EoS are more complex than the ideal gas EoS and lead to more complex models.

The main goal of the present work is to perform numerical investigations of non-equilibrium condensing flows of non-ideal single phase gases, under high-pressure conditions in a laval nozzle. The main objective is to verify whether well known nucleation rate and growth rate models available can accurately predict the occurrence of condensation under such conditions.

The open-source code Stanford University Unstructured (SU2) has been updated to allow the use of non-ideal gas models for compressible fluid flows Vitale *et al.* (2015), which made the code suitable for such studies. Furthermore, researchers from TU Delft have implemented condensation models on a branch, *feature_2phase* Azzini (2019), of the SU2 code. For those reasons, and because open source codes are free for use and open to contributions, this branch has been chosen to perform the necessary simulations for the present paper.

2. METASTABLE CONDENSATION OF NON-IDEAL COMPRESSIBLE FLUIDS

2.1 Nucleation and growth rate models

The modeling of condensation phenomena consists in choosing a method to evaluate the evolution of the liquid phase, such as the method of moments, and appropriate models for the nucleation (J) and growth rates of liquid droplets (G). The former is related to the number of clusters with critical size (r_c) that are formed per unit volume, whereas the latter refers to the rate at which theses clusters grow.

In high speed flows, such as laval nozzles, condensation occurs under metastable conditions, which means that the liquid phase does not form readily after the saturation line is crossed. The flow continues to expand isentropically, the vapor becomes supersaturated, up to a certain point where the phase change is triggered. This point is known as the Wilson point Azzini (2019); Lettieri *et al.* (2017), which lies between the saturation and spinodal lines. This is owed to the high speed flow, vapour molecues simply cannot rearrange themselves and change phase quickly enough under such conditions. Additionally, liquid cluster are unstable until they reach a critical size (r_c). Hence, if these clusters are below the critical size they tend to re-evaporate, whereas if they are greater than the critical they tend to grow. This is the reason why only clusters with sizes that are greater than or equal to the critical size grow to form the liquid phase Bakhtar *et al.* (2005).

Figure illustrates how condensation occurs in such flows. The vapor phase expands isentropically and crosses the saturation line, point II. At this point no phase change occurs and the flow further expands until it reaches point III, also known as Wilson point, where condensation occurs. Points II and III define the metastable region and in this region the flow is said to be metastable.

The main nucleation mechanism in such flows is the homogeneous one. Therefore, the models developed for the condensation of liquid phase in high speed gas are entirely based on the theory of homogeneous nucleation. The nucleation rate, denoted by J, can be written in the following general form

$$J = \left(\frac{1}{1+\Phi}\right) q_c \frac{\rho_g^2}{\rho_l} \left(\frac{2\sigma}{\pi m^3}\right) \exp\left(-f\frac{4\pi\sigma}{3kT_v} r_c^2\right) \tag{1}$$

where q_c is the condensation coefficient, usually taken to be equal to unity, ρ_v is the vapor density, ρ_l is the liquid density, σ is the surface tension, m is the mass of a molecule, k is the Boltzmann constant, T_v is the vapor temperature, f is a correction factor, and r_c is the critical radius.

If Φ is set to zero and f to unity, then one obtains the so-called classical nucleation rate model, which was the first condensation theory and is commonly referred to as the Classical Nucleation Theory (CNT) Bakhtar *et al.* (2005). This

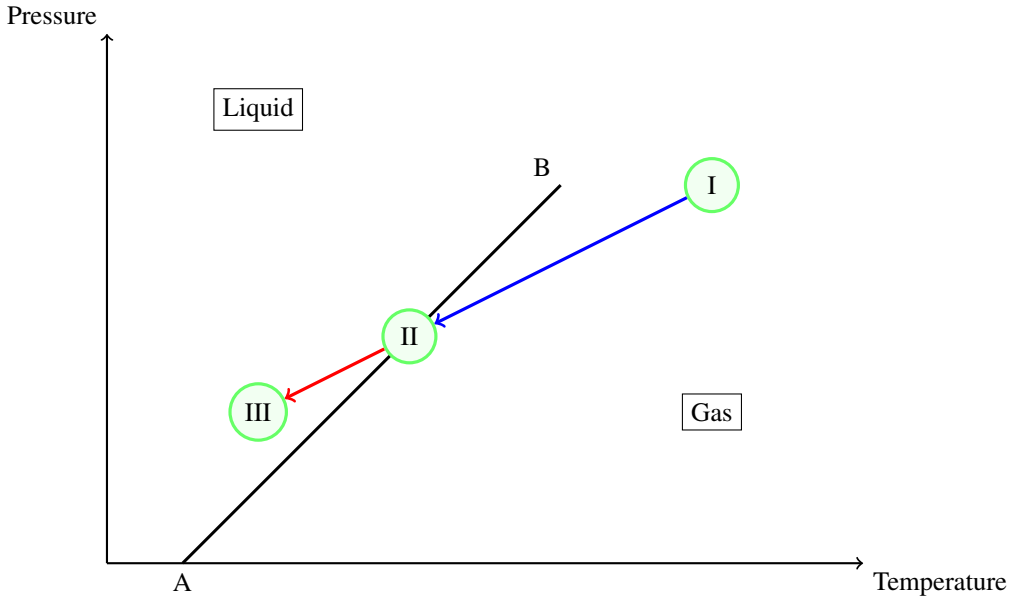

Figure 1. Schematic representation of the thermodynamic process involved in ondensation.

theory assumed thermodynamic equilibrium, in which both phases were assumed to have the same temperature.

If f equals unity and Φ is equal to the following expression

$$\Phi = 2\left(\frac{\gamma-1}{\gamma+1}\right)\frac{H_{lv}}{RT_v}\left(\frac{H_{lv}}{RT_v}-\frac{1}{2}\right) \tag{2}$$

where γ is the ratio of specif heats, R is the gas constant, H_{lv} is the difference between the vapor and liquid enthalpies, $H_v - H_l$, where H_v and H_l are the vapor and liquid enthalpies, respectively, one obtains the so-called Non-Isothermal correction Azzini (2019); Bakhtar *et al.* (2005). From the name it is clear that the previous assumption of thermodynamic equilibrium between the liquid and vapor phases has been dropped.

Additionally, by setting Φ equal to the expression in equation (2) and $f = 1.33$, one obtains the factor f correction, which has been reported to provide the best results for the condensation of wet-steam under low pressure conditions Starzmann *et al.* (2018).

The critical radius is derived from the Gibbs free energy expression for the formation of a liquid droplet. For a vapor with non-ideal behavior the critical radius expression is given by Hric and Halama (2016)

$$r_c = \frac{2\sigma}{\rho_l(RT_v lnS + \Delta G_r) - (P_v - P_{sat})} \tag{3}$$

where S is the supersaturation rate, which expresses the ratio between the vapor pressure and the vapor saturation pressure calculated at the vapor temperature T_v, and is given by Azzini (2019); Bakhtar *et al.* (2005)

$$S \equiv \frac{P_v}{P_{sat}(T_v)} \tag{4}$$

The term ΔG_r in equations (3) is the is the difference in residual specific Gibbs free energy between the vapor and the saturated vapor Hric and Halama (2016)

$$\Delta G_r = G_r(P_v, T_v) - G_r(P_{sat}, T_v) \tag{5}$$

As for the droplet growth rate, the models available in the literature are derived from kinetic theory of gases. A thorough discussion of such models is beyond the scope of the present paper and the interested reader may refer to Peeters *et al.* (2001) for further details on such models. Azzini (2019) implemented the Gyarmathy model on the SU2 branches *feature_2phase* and *feature_turbo2phase*, which is given by

$$G = \frac{\kappa_v(Tsat(P_v) - T_v)(1 - r_c/r)}{\rho_l H_{lv}[r + (1-\nu)\frac{\lambda_v}{Pr}]} \tag{6}$$

where Pr is the Prandtl number, r is the droplet radius, κ_v is the thermal conductivity of the vapor phase, and λ_v is given by

$$\lambda_v = 1.5\frac{\mu_v\sqrt{RT_v}}{P_v} \tag{7}$$

where μ_v is the viscosity of the vapor phase. Note that ν in equations (6) is only a term from eq. (6) that should not be confused with the kinematic viscosity. Its value is given as follows

$$\nu = \frac{RT_{sat}(P_v)}{H_{lv}}\left[\frac{1}{2} - \frac{1}{4}\left(\frac{\gamma+1}{\gamma-1}\right)\frac{RT_{sat}(P_v)}{H_{lv}}\right] \tag{8}$$

where $T_{sat}(P_v)$ is the saturation temperature calculated at the vapor pressure P_v.

2.2 The method of moments

Apart from the nucleation and growth rates models, it is necessary to evaluate the evolution of the liquid phase. One such possibility is the so-called Hill's method of moments Hill (1966), which applies the method to estimate quantities relevant to the study of condensation phenomena, e.g., the total number of liquid droplets per unit volume (moment of order zero), the average droplet radius (moment of order one), the total liquid surface (moment of order two), and the total liquid volume (moment of order three). The moment equations are calculated in addition to the conservation equations.

A total of three moment equations plus a normalization condition, which is the moment of order zero, are required. The third order moment is needed since it is related to the liquid mass fraction. The previous two moments are also needed due to the fact that the moment equations are calculated recursively. Thus, the method of moments require four extra equations to be added to the original conservation equations. A comprehensive discussion of this method can be found in Put (2003); Hagmeijer (2004).

For the simulation of condensation phenomena, there are two possibilities to write the conservation equations, as reported in the literature Dykas and Wróblewski (2011). The first one is called Single-Phase model in which the liquid and vapor phases are analyzed together and averaged values of density, temperature, pressure and so forth are calculated. In this case, neither of the original conservation equations require source terms.

It is also possible to analyze the liquid and vapor phases separately. Such approach is termed Two-Phase model. In this case, the conservation equations have source terms to account for the formation of the liquid phase and for the heat transferred from the liquid phase to the vapor phase in the form of enthalpy H_{lv}. Since the Two-Phase model is the one available on the SU2 branches more emphasis will be given to this model.

The conservation equations for the vapor phase, for a two-dimensional Euler problem, can be written in conservation form as follows

$$\frac{\partial \mathbf{U}}{\partial t} + \frac{\partial \mathbf{F}_x}{\partial x} + \frac{\partial \mathbf{F}_y}{\partial y} = \mathbf{S} \tag{9}$$

where

$$\mathbf{U} = \begin{bmatrix} \rho_v \\ \rho_v u \\ \rho_v v \\ \rho E_{0,v} \end{bmatrix}; \mathbf{F}_x = \begin{bmatrix} \rho_v u \\ \rho_v u^2 + P \\ \rho_v uv \\ H_{0,v} u \end{bmatrix}; \mathbf{F}_y = \begin{bmatrix} \rho_v v \\ \rho_v uv \\ \rho_v v^2 + P \\ H_{0,v} v \end{bmatrix}; \mathbf{S} = \begin{bmatrix} S_v \\ S_v u \\ S_v v \\ S_v H_{0,l} \end{bmatrix}; \tag{10}$$

and S_v is given by Azzini (2019)

$$S_v = -\rho_m \frac{3y}{R}\frac{\partial R}{\partial t} \tag{11}$$

where ρ_m is an average between the vapor and liquid densities, given by

$$\rho_m = \frac{1}{y/\rho_l + (1-y)/\rho_v} \tag{12}$$

where y is the liquid mass fraction, R is the droplet average radius and $\partial R/\partial t$ is the variation of the average droplet radius with respect to time Azzini (2019).

The moment equations for the liquid phase can also be written in conservation form as follows

$$\frac{\partial \mathbf{W}}{\partial t} + \frac{\partial \mathbf{H}_x}{\partial x} + \frac{\partial \mathbf{H}_y}{\partial y} = \mathbf{S}_\mu \tag{13}$$

where

$$\mathbf{W} = \begin{bmatrix} \rho_m \mu_0 \\ \rho_m \mu_1 \\ \rho_m \mu_2 \\ \rho_m \mu_3 \end{bmatrix}; \mathbf{H}_x = \begin{bmatrix} \rho_m \mu_0 u \\ \rho_m \mu_1 u \\ \rho_m \mu_2 u \\ \rho_m \mu_3 u \end{bmatrix}; \mathbf{H}_y = \begin{bmatrix} \rho_m \mu_0 v \\ \rho_m \mu_1 v \\ \rho_m \mu_2 v \\ \rho_m \mu_3 v \end{bmatrix}; \mathbf{S}_\mu = \begin{bmatrix} \rho_m J \\ \rho_m J r_c + \mu_0 G \\ \rho_m J r_c^2 + \mu_1 G \\ \rho_m J r_c^3 + \mu_2 G \end{bmatrix}; \tag{14}$$

where the variables μ_n are defined as follows Hagmeijer (2004); Put (2003)

$$\mu_n \equiv \langle r^n \rangle \equiv \int_{-\infty}^{+\infty} r^n f(\mathbf{x}, r, t) dr \tag{15}$$

where r is the droplet radius, $\mathbf{x}$ represents the spatial coordinates, t is the time coordinate, and $f(\mathbf{x}, r, t)$ is the droplet radius distribution function Hagmeijer (2004); Put (2003). Note that $(\mathbf{x}, r)$ represents a phase-space.

Since r is a non-negative quantity, the lower bound of the integral in equation (15) can be set to zero. Thus

$$\mu_n \equiv \langle r^n \rangle \equiv \int_{0}^{+\infty} r^n f(\mathbf{x}, r, t) dr \tag{16}$$

Note that the variables μ_n are not the moments of the distribution function $f(\mathbf{x}, r, t)$. For the μ_n to be the actual moments, the distribution f would have to be normalized, so that it would be an actual PDF, that is, a Probability Density Function. In order to obtain these quantities, the variables μ_n must be normalized with respect to the normalization condition, namely the μ_0. Hence the moments M_n of $f(\mathbf{x}, r, t)$ are given by

$$M_n \equiv \frac{\mu_n}{\mu_0} \tag{17}$$

The conservation and moment equations are weakly coupled and the liquid temperature is evaluated by using the capillarity model, which is given by Azzini (2019)

$$T_l = T_{sat}(P) - (T_{sat}(P) - T_v)\frac{r_c}{R} \tag{18}$$

The liquid and vapor phases are assumed to be kinematic equilibrium, i.e.,their velocity fields are also the same Azzini (2019). The mechanical equilibrium hypothesis is also employed by Dykas and Wróblewski (2011).

3. RESULTS

3.1 Numerical setup

The simulations of wet-steam condensation under high pressure conditions were performed for a two-dimensional Euler problem. Roe's upwind scheme Roe (1981) was applied to the conservation equations and Rusanov's flux Rusanov (1961) was applied to the moment equations. The mesh employed in the simulations is an unstructured one which has around 25k elements and the working fluid is wet-steam for all simulations to be presented in this section.

Section 3.2 discusses briefly the results of flow fields obtained for different equations of state (EoS). The main objective was to compare how the numerical results may be affected by the choice of the EoS chosen. This study did not take condensation phenomena into account. Condensing flows are discussed in section 3.3 , where a simulation of condensation under high pressure condition was performed and the relevant parameters, e.g., the moments, the liquid mass fraction, etc, are presented. The working fluid in both sections is steam - dry steam in section 3.2 and wet-steam in section 3.3

The numerical simulations were performed with the branch *feature_2phase* of the open-source code Stanford University Unstructured (SU2), which has been implemented with an external thermodynamic library by researchers from TU Delft and can be found in the SU2 git repositories Azzini (2018). For further details on the branch, the reader may refer to Azzini (2019) This library allows for the use of more complex thermodynamic models and equations of state, e.g., RefProp, necessary for the investigation.

3.2 Analysis of the effect of the equation of state in high pressure compressible flows

This section presents a comparison between the flow of dry-steam, i.e., absence of condensation, using three equations of state: the ideal gas, Peng-Robinson-Strjek-Vera (PRSV), and the improved Peng-Robinson-Strjek-Vera models (iPRSV). In all three cases the same boundary conditions $P_0 = 100.7$ bar, $T_0 = 638.38$ K, and a back pressure (P_b) of $0.25P_0$ were employed. The main goal was to verify variation of the flow properties with respect to the equation of state (EoS) adopted.

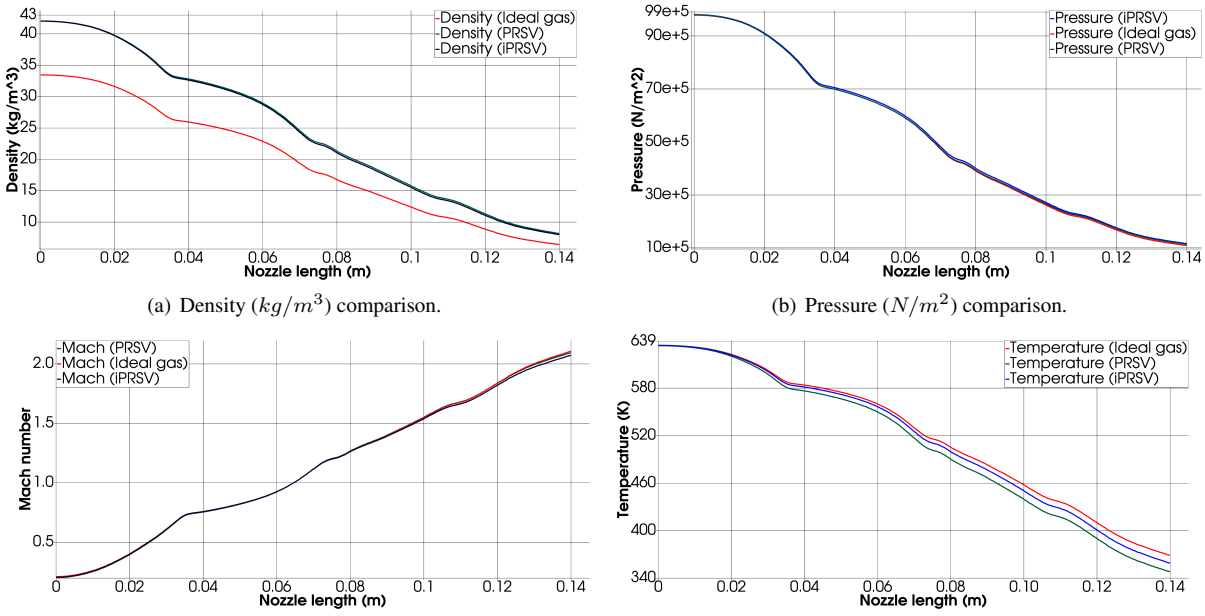

(a) Density (kg/m^3) comparison.

(b) Pressure (N/m^2) comparison.

(c) Mach number comparison.

(d) Temperature (K) comparison.

Figure 2. Comparison between the density 2(a), pressure 2(b), Mach number 2(c), and temperature 2(d) obtained using the ideal gas (red line), PRSV (green line), and iPRSV (blue line) models. The lines were plotted with respect to the centerline of the nozzle.

Figures 2(a) to 2(d) show how the flow properties vary with different EoS. The most affected properties were clearly the density 2(a) and temperature 2(d). The pressure as well as the Mach number did not vary significantly with the EoS adopted. In view of the differences among the various EoS, in particular of the ideal gas equation with respect to the others, it can be concluded that for such high pressure conditions in which $P_v/P_c \approx 0.458$, where P_v and P_c are the vapor pressure and the critical pressure, respectively, and considering $Pc \approx 200$ bar, this EoS is not suitable for the present analysis since the use of such EoS could lead to inaccurate results.

Hence, it can be said that high pressure flows are more complex than low pressure ones since the ideal gas model does not provide sufficiently accurate results, and the assumptions that the gas is thermically and calorically perfect may not hold. Figure 3(c), for example, show that the ratio of specific heats vary from approximately 1.95 to 1.45, which is by no means a negligible variation. Though the stagnation conditions used to obtain the figure 3(c) were different from those used for figure 2, it illustrates the fact that such hypothesis no longer hold under high pressures, and therefore more sophisticated models and hypothesis are needed in order to simulate accurately such flows.

In spite of the better results provided by non-ideal EoS, they increase the complexity of the problem, and likely the computational cost as well. As an example, with the ideal gas model, using two cores, between $80 - 120$ iterations per minute were performed. When attempting to use the NIST's RefProp, with two cores, the performance dropped drastically to $4 - 6$ iterations per minute. Hence, the more sophisticated the model, the better, i.e., more accurate, it tends to be. However, it is not only the EoS that is being changed, but also the way thermodynamic properties such as enthalpy, entropy, and so forth are evaluated - which is related to the sharp increase in computational cost.

All models have their pros and cons and it is important to known the capabilities and limits of all these models in order to perform efficient numerical simulations. Sophisticated models such as NIST's RefProp are among the best ones. However, depending on the boundary conditions, if the different models are only slightly different, then these highly sophisticated models may not be suitable owing to their high computational cost. Thus, knowledge of such models and their validity is useful in order to choose which of them is best for a given problem, so as to performing efficient numerical simulations.

3.3 Analysis of condensation phenomena under high pressure conditions

A simulation of condensing flows using the nozzle geometry of Moses and Stein (1978) was performed with the boundary conditions set to $P_0 = 148.1$ bar, $T_0 = 668.87$ K, and a back pressure (P_b) of $0.25P_0$. These conditions were based on the experimental study of Gyarmathy (2005). The equation of state employed was the iPRSV. The nucleation rate employed was the Non-isothermal correction and the growth rate model was that of Gyarmathy Azzini (2019).

Figure 3 shows the results of condensation of wet-steam under high pressures. It can be seen from figure 3(a) that the onset of nucleation resembles a Dirac Delta function that occurs shortly after the nozzle throat, which is located around $x \approx 0.0622$ m. From figure 3(b), it can be seen that liquid droplets start growing slightly before the condensation onset,

where the growth rate of liquid droplets reaches a maximum value, and then decrease abruptly. Note that even though the nucleation rate quickly reaches a peak and the drops to zero, the growth rate decreases but does not reach zero, meaning that the liquid droplets keep on growing, though at a slower rate. This statement is supported by figures 4(b) and 5(a) from where it can be seen that the average radius as well as the liquid mass fraction, respectively, increase after the condensation onset.

Figure 3(c) shows the variation of the ratio of specific heats γ along the length of the nozzle. It can be seen that for such boundary conditions the vapor phase is not calorically perfect, hence the variation of γ. It also indicates that the vapor phase is far from the perfect gas behavior, which is supported by figure 5(b) where it can be seen that the compressibility factor is around 0.74 at the nozzle inlet and then grows to nearly 0.91 at the outlet. For the gas to be considered ideal, this factor would have to be around unity. Thus, up until around $x \approx 0.11$ the gas cannot be regarded as ideal. Additionally, the hypothesis of constant γ may not be applied to high pressure flows given the variations of around 25.64% in the values of gamma, see figure 3(c), since such hypothesis may lead to inaccurate results.

Figures 4(a) to 4(d) show moments obtained for the simulation. As it has been mentioned earlier, this moments are related to the evolution of the liquid phase. It can be seen from figure 4 that the liquid phase does not appear until the divergent section of the nozzle, where the flow is supersonic and the conditions for condensation are met. As the flow expands, both pressure and temperature decrease, whereas the Mach number increases. This proceeds until the Wilson temperature, which is the trigger for metastable condensation, is reached. The phase change then occurs as a wavefront after the throat of the nozzle.

Figure 4(a) shows that the total number of droplets per unit volume is higher near the condensation onset and drops as the flow moves downstream. By comparing it with figures 4(b), 4(c), 4(d), and 5(a), which show that the average droplet radius, total liquid surface, the total liquid volume, and the liquid mass fraction, it can be concluded most liquid droplets are located near the condensation onset. These droplets are initially small and, as one moves downstream, there are fewer but bigger droplets, since their average radius grows in the downstream direction, see figures 4(b) through 4(d). Thus, it can be concluded that there are two parts in the condensation process: the first one is the formation of liquid droplets whereas the second is related to their growth.

Figure 5(a) shows the evolution of the liquid mass fraction along the nozzle. It can be seen that it grows from zero to approximately 0.17 at the nozzle outlet, which is consistent with the moment of order three 4(d) which show that the total liquid volume increases downstream of the throat of the nozzle.

Figures 3(c) and 5(b) illustrate and are in agreement with the discussion of the previous section. They indicate that when the pressures are sufficiently high, in this case $P_v/P_c \approx 0.673$, the assumption that the ratio of specific heats is constant is not suitable. Furthermore, the hypothesis of ideal behavior are also unsuitable given that the compressibility factor is far from unity until $x \approx 0.11$ m, which is close to the outlet of the nozzle. Consequently, through most part of the flow, the gas shows non-ideal behavior, which justifies the use of non-ideal gas models for such simulations.

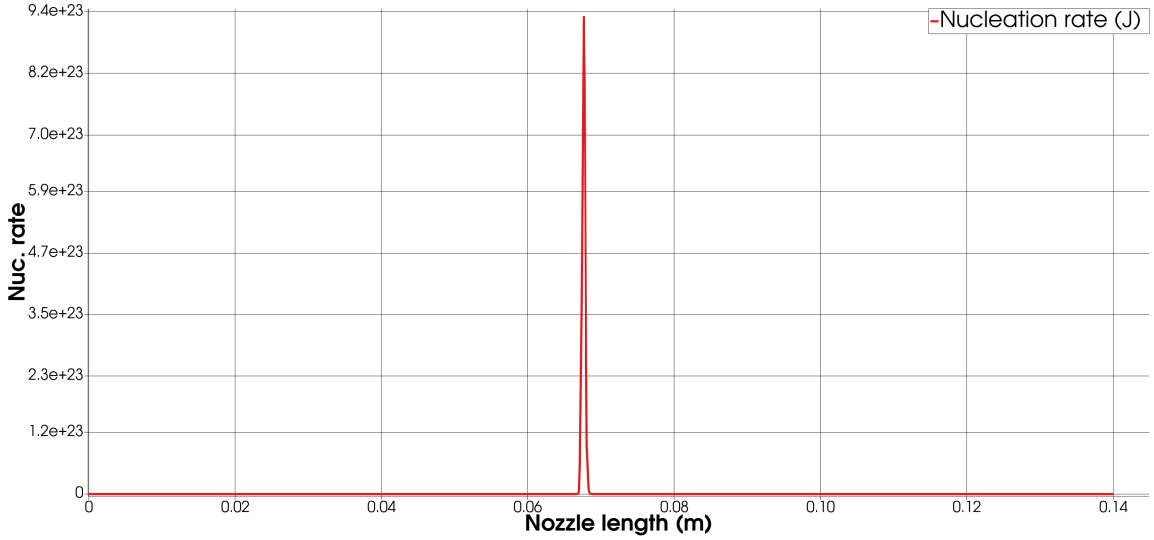

(a) Nucleation rate.

(b) Growth rate.

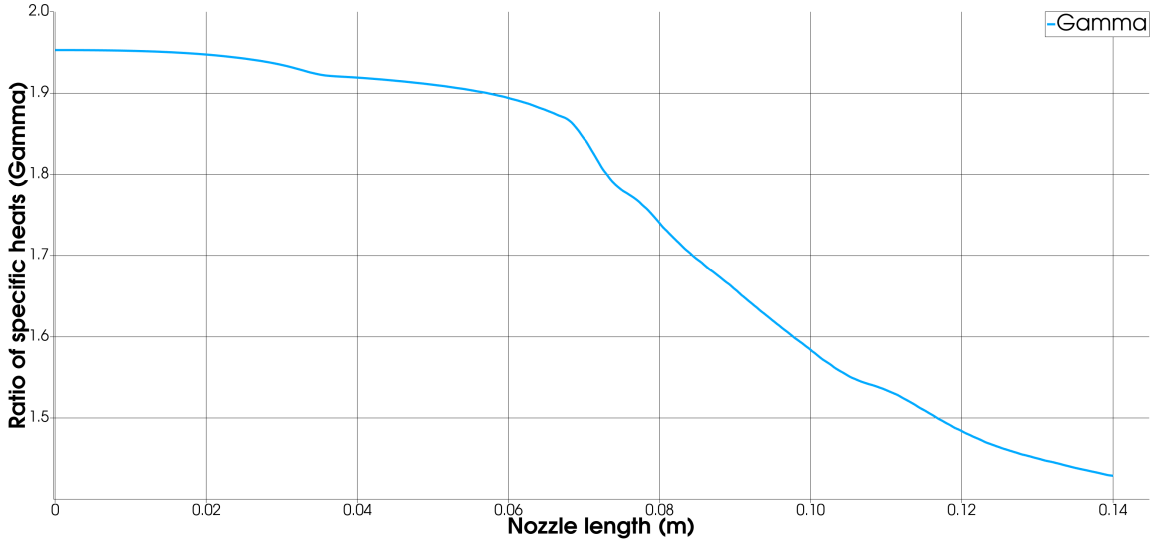

(c) Variation of γ.

Figure 3. Nucleation rate 3(a), growth rate 3(b), and the variation of γ along the length of the nozzle over the center line, obtained for wet-steam condensation using the iPRSV EoS, for $P_0 = 148.1$ bar, $T_0 = 667.87$ K and a back pressure equal to $0.25P_0$. The curves were plotted with respect to the centerline of the nozzle.

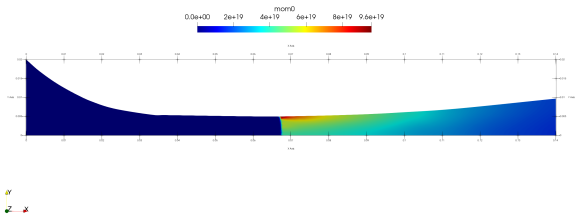

(a) Moment of order zero.

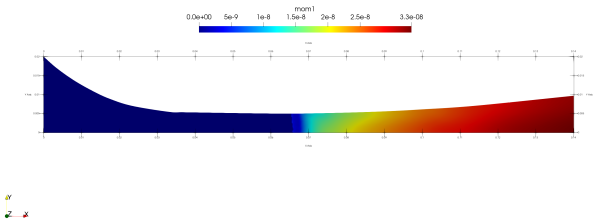

(b) Moment of order one.

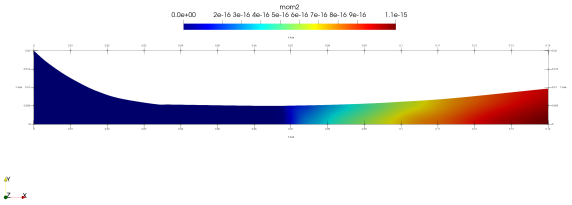

(c) Moment of order two.

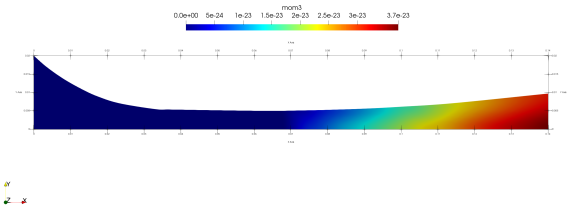

(d) Moment of order three.

Figure 4. Moments of order zero 4(a), one 4(b), two 4(c), and three 4(d) obtained for wet-steam condensation using the iPRSV EoS, for $P_0 = 148.1$ bar, $T_0 = 667.87$ K and a back pressure equal to $0.25P_0$.

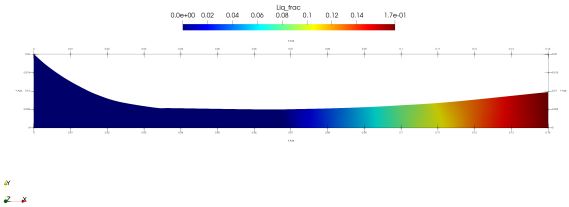

(a) Liquid fraction of water which condensed in the nozzle.

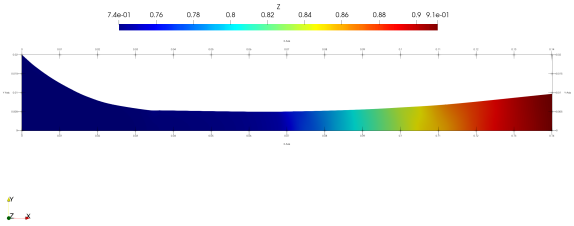

(b) Compressibility factor (Z).

Figure 5. Liquid fraction of water 5(a) and compressibility factor 5(b) along the nozzle. The thermodynamic model used was the iPRSV EoS, with $P_0 = 148.1$ bar, $T_0 = 667.87$ K and back pressure equal to $0.25P_0$.

3.4 Ideal vs Non-ideal models for high pressure condensation

Section 3.2 presented a comparison between the numerical results obtained for the ideal gas EoS and for the PRSV EoS in the absence of condensation. This section aims at investigating how the choice of the equation of state affects the prediction and accuracy of the numerical results.

The geometry, the boundary conditions, and the mesh employed for the simulations were the same as those of the previous section. The ideal gas and the PRSV EoS were chosen to perform the comparisons.

Figure 6 shows the comparison between the nucleation rate obtained using the ideal gas model and the PRSV EoS, figure 6(a), as well as a comparison between the average radius (or first order moment) obtained for the same models, figure 6(b).

From figure 6(a) it can be seen that for the ideal gas model the position of the nucleation rate, which is related to the condensation onset, differs considerably from the results obtained with PRSV. Note that not only is the position of the nucleation rate different, further downstream, but also its magnitude is greater than that obtained for the PRSV EoS.

Figure 6(b) shows a comparison between the droplet radius along the length of the nozzle. As was seen in figure 6(a), the ideal gas model predicts that the first order moment begins to grow at around $x \approx 0.09$ m whereas the PRSV model predicts that this should occur at $x \approx 0.08$ m. In addition, the ideal gas model predicts smaller droplet radius than the PRSV model. Again, for the ideal gas model the condensation onset occurs further downstream, closer to the nozzle outlet, than it should.

From figures 6(a) and 6(b), it can be concluded that for the ideal gas model the phase change occurs further downstream than the PRSV model and the magnitudes of the droplet radius and nucleation rate differ between the two models. Upon considering that these simulations were performed with a high stagnation pressure of 100.7 bar, it is likely that the PRSV model is more accurate results than the ideal gas model.

For low-pressure condensing flows, some simplifying hypothesis are made. As an example, it is common to assume, in the derivation of the critical radius expression, that the metastable vapor behaves as an ideal gas. The expression thus obtained is somewhat simpler than equation (3) Bakhtar *et al.* (2005). Such hypothesis may be used for low-pressure condensing flows, in order to simplify the calculations involved without compromising the accuracy of the simulation. However, from the results shown it can be seen that as pressure increases the vapor phase moves away from the ideal behavior and consequently the results obtained with ideal gas models are quite different from those obtained with non-ideal gas models.

3.5 Metastable condensation in high-speed nozzle flows

In high-speed nozzle flows the vapor phase expands isentropically until it crosses the saturation line. This, however, does not result in immediate phase change, and the vapor continues to expand isentropically beyond the saturation line up

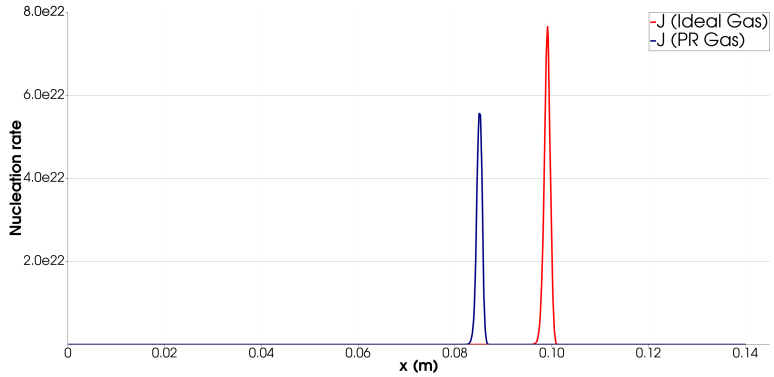

(a) Comparison between the nucleation rate obtained with the ideal gas model and the PRSV.

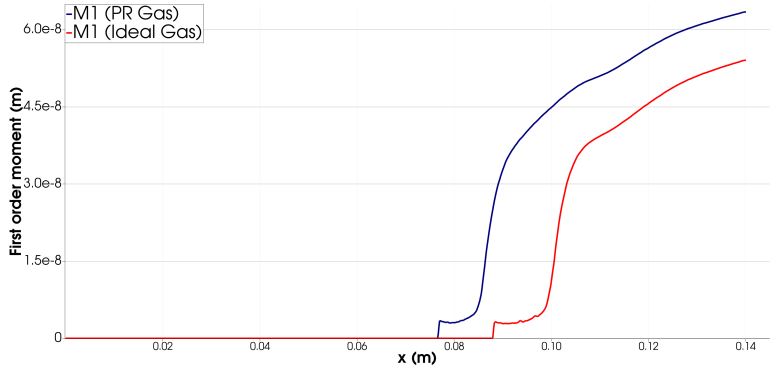

(b) Comparison between the first order moment, i.e., the average droplet radius, for the ideal gas model and the PRSV EoS.

Figure 6. Comparison between the zeroth 6(a) and first order moments 6(b) obtained for the the ideal gas model (red lines) and the Peng-Robingson-Strjek-Vera EoS (blue lines) plotted along the length of the nozzle.

until a certain point, the so-called Wilson point, where condensation effectively occurs Azzini (2019). Once the saturation line is crossed the vapor becomes supersaturated and enters the metastable state where it remains until condensation occurs Azzini (2019).

One way to evaluate metastability and the metastable region (or domain) is by analyzing the supersaturation ratio, which is defined in equation (4). If $S = 1$ the vapor is in equilibrium condition. If $S > 1$, it is supersaturated and condensation may occur. Finally, if $S < 1$ condensation does not occur and any liquid phase that may be present must re-evaporate Azzini (2019); Bakhtar *et al.* (2005). Note that despite the fact that S shows the metastable region, it does not tell whether nor when phase change occurs. It provides information regarding the flow region where phase change is possible and where it is not. In order to obtain information regarding the position of the condensation onset one must determine where the flow crosses the Wilson line.

Figure 7 shows the supersaturation rate for obtained for Moses and Stein (1978) nozzle, with the nozzle throat being located at $x = 0.0622$ m, on the left axis. The right axis shows the zeroth order moment, and the x axis represents the length of the nozzle.

A mesh of around 50k elements was used. The stagnation pressure and temperature were set to $P_0 = 100.7$ bar and 615 K, respectively. The supersonic outlet condition and the PRSV EoS were employed in this simulation.

It can be seen from figure 7 that S is less than unity in the convergent part of the nozzle, which is consistent with the physics of condensation, since the phase change only occurs in the divergent section where the flow is supersonic. After the nozzle throat S increases rapidly and becomes greater than unity at approximately $x \approx 0.07$ m. The supersaturation ratio remains greater than unity in the interval $0.07 < x < 0.09$. It can be said that this region represents the metastable domain of the flow. Moreover, despite being thin, the domain of metastability cannot be neglected or assumed to the so thin that it does not affect the flow.

From figure 7 it can be seen that condensation occurs inside the metastable region. Furthermore, it can also be seen that the condensation onset is located inside the metastable region near the maximum value of S. Note that shortly after the occurrence of phase change S drops to values near unity, which means that after condensation the flow moves towards an equilibrium state. Also, the number of droplets per unit volume (zeroth order moment) decreases as the flow moves away from the metastable state towards equilibrium.

Figure 7(b) shows how the supersaturation ratio varies along the nozzle. $S_r = 1$ corresponds to the yellow color and

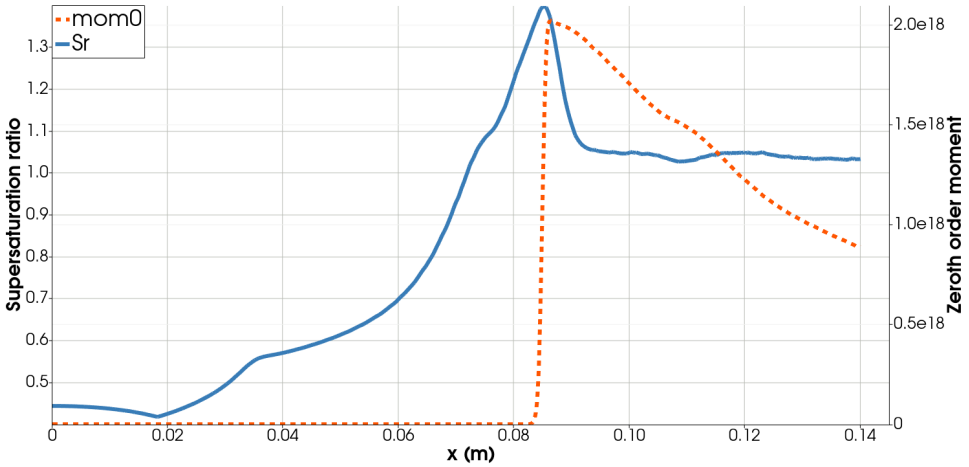

(a) Fluctuations in the supersaturation rate (blue line) and zeroth order moment (orange dashed line) plots along the length of the nozzle with respect to the centerline.

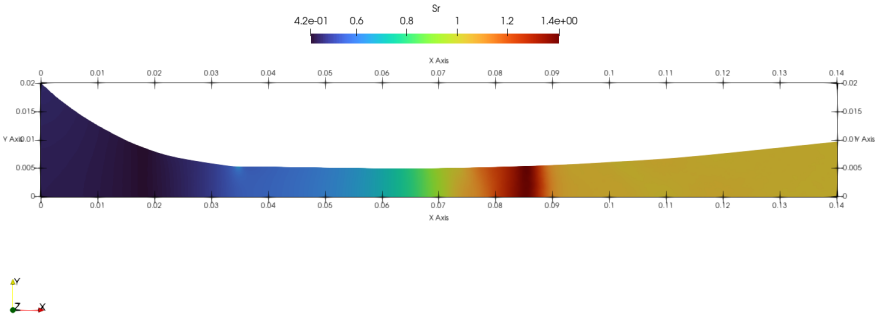

(b) Supersaturation rate alo.

Figure 7. 7 Supersaturation (blue line) and zeroth order moment (orange dashed line) plots along the length of the nozzle. These plots were taken with respect to the centerline. 7(b) variation of the supersaturation ratio along the nozzle.

the orange and red colors correspond to $S_r > 1$, i.e., the metastable region. As both figures 7(a) and 7(b) indicate, though this region is thin it is not negligible. Also, since high-speed condensation occur with respect to the Wilson line instead of the saturation line Azzini (2019); Bakhtar *et al.* (2005); Lettieri *et al.* (2017), ignoring this region would likely result in accuracy loss since the models would predict condensation occurring at an earlier position.

4. CONCLUSIONS

High-speed condensation phenomena must take into account the effects of metastability owing to the fact that for such flows the phase change occurs with respect to the Wilson line instead of the saturation line Azzini (2019); Bakhtar *et al.* (2005). This is a consequence of the vapor expanding beyond the saturation line. As analyzed in section 3.5 , the metastable region may be represented by the supersaturation ratio and from figure 7 it can be seen that condensation occurs within it. Therefore, metastability should be taken into account in such high-speed condensing flows.

For high-speed flows under high pressure conditions should take into account not only metastability but non-ideal gas behavior as well. As discussed in sections 3.2 and 3.4 , the results thus obtained show that the flow properties cannot be accurately modeled with the ideal gas model if the flow is subjected to high pressure conditions. The discrepancies between the results obtained for the ideal gas EoS and other non-ideal gas models, such as the PRSV EoS, as well as the compressibility factor, shown in figure 5(b), are clear evidences the ideal models are not suitable for such simulations. Furthermore, these differences in the flow properties lead to discrepancies in the prediction of the condensation onset in such flows, thus affecting the accuracy of the simulations. Therefore, other models which can describe accurately non-ideal gas behavior should be emplyed for high-speed condensing flows under high-pressure conditions.

As for non-ideal gas behavior, the discussion is quite complex. An equation of state as well as models to evaluate thermodynamic properties such as the specific heat under constant pressure, the fluid entropy, and so forth are required.

Several models are available to represent such behavior. Some are based on cubic EoS whereas others are based on semi-empirical EoS. In addition, several of these models lose their accuracy as the critical point of the fluid is approached. In such cases, robust equations of state or thermodynamic libraries, e.g., NIST's REFPROP, are required. These models are reported to be the most accurate ones specially near the critical point. One disadvantage of such models is their high computational costs when compared with other EoS.

Accurate simulations of non-ideal gas flows under high-pressure conditions require both accuracy and efficiency. As previously stated, models such as REFPROP are considered to be among the best ones currently available. However, it is also important to take into account the computational cost of the simulations. As an example, one may choose a simpler non-ideal gas model whose computational cost is less than the more complex ones if this does not lead to a sharp drop in accuracy. In other cases, such as flows near the critical point of the fluid, require the use of more complex and accurate thermodynamic models even if they have a high computational cost.

The study of non-ideal gas behavior is an important one not only for developing a better understanding of such flows but also to provide the necessary information about each of these models. When a simpler model may be employed without considerable accuracy losses, when simplifying ideal gas hypothesis may be employed are important questions an engineer needs to answer in order to perform accurate numerical simulations but without unnecessarily increasing their computational costs. Such knowledge will only be available by conducting more researches in the topic of non-ideal gas behavior.

5. ACKNOWLEDGEMENTS

The authors gratefully acknowledge support of the RCGI – Research Centre for Gas Innovation, hosted by the University of São Paulo (USP) and sponsored by FAPESP – São Paulo Research Foundation (2014/50279-4) and Shell Brasil, and the strategic importance of the support given by ANP (Brazil's National Oil, Natural Gas and Biofuels Agency) through the R&D levy regulation. The authors would also like to thank Conselho Nacional de Desenvolvimento Científico e Tecnológico, CNPq, for the M.S. scholarship for the first author. The authors further acknowledge the partial support for the present research provided by CNPq under the Research Grant No. 309985/2013-7.

6. REFERENCES

Azzini, L., 2018. "SU2-feature_2phase". https://github.com/su2code/SU2/tree/feature_2phase.

Azzini, L., 2019. *Numerical Investigation Of Dense Condensing Flows For Next-Generation Power Units*. Ph.D. thesis, Delft University of Technology. doi:10.4233/uuid:6c84e51e-4111-4638-ae70-24a510db3ca5.

Bakhtar, F., Young, J., White, A. and Simpson, D., 2005. "Classical nucleation theory and its application to condensing steam flow calculations". *Proceedings of The Institution of Mechanical Engineers Part C-journal of Mechanical Engineering Science - PROC INST MECH ENG C-J MECH E*, Vol. 219, pp. 1315–1333. doi:10.1243/095440605X8379.

Dykas, S. and Wróblewski, W., 2011. "Single- and two-fluid models for steam condensing flow modeling". *International Journal of Multiphase Flow*, Vol. 37, No. 9, pp. 1245–1253. ISSN 0301-9322. doi:https://doi.org/10.1016/j.ijmultiphaseflow.2011.05.008. URL https://www.sciencedirect.com/science/article/pii/S0301932211001157.

Gyarmathy, G., 2005. "Nucleation of steam in high-pressure nozzle experiments". *Proceedings of the Institution of Mechanical Engineers, Part A: Journal of Power and Energy*, Vol. 219, No. 6, pp. 511–521. doi:10.1243/095765005X31388. URL https://doi.org/10.1243/095765005X31388.

Hagmeijer, R., 2004. "Equivalence of two different integral representations of droplet distribution moments in condensing flow". *Physics of Fluids*, Vol. 16, No. 1, pp. 176–183. doi:10.1063/1.1630052. URL https://doi.org/10.1063/1.1630052.

Hill, P.G., 1966. "Condensation of water vapour during supersonic expansion in nozzles". *Journal of Fluid Mechanics*, Vol. 25, No. 3, pp. 593-620. doi:10.1017/S0022112066000284.

Hric, V. and Halama, J., 2016. "Performance of simple condensation model in high-pressures". In *TOPICAL PROBLEMS OF FLUID MECHANICS*. doi:10.14311/TPFM.2016.009.

Lettieri, C., Paxson, D., Spakovszky, Z. and Bryanston-cross, P., 2017. "Characterization of non-equilibrium condensation of supercritical carbon dioxide in a de laval nozzle". *Journal of Engineering for Gas Turbines and Power*, Vol. 140. doi:10.1115/1.4038082.

Moses, C.A. and Stein, G.D., 1978. "On the Growth of Steam Droplets Formed in a Laval Nozzle Using Both Static Pressure and Light Scattering Measurements". *Journal of Fluids Engineering*, Vol. 100, No. 3, pp. 311–322. ISSN 0098-2202. doi:10.1115/1.3448672. URL https://doi.org/10.1115/1.3448672.

Peeters, P., Luijten, C. and van Dongen, M., 2001. "Transitional droplet growth and diffusion coefficients". *International Journal of Heat and Mass Transfer*, Vol. 44, No. 1, pp. 181–193. ISSN 0017-9310. doi:https://doi.org/10.1016/S0017-9310(00)00098-3. URL https://www.sciencedirect.com/science/article/pii/S0017931000000983.

Put, F., 2003. *Numerical Simulation Of Condensation In Transonic Flows*. Ph.D. thesis, Universiteit Twente.

Roe, P., 1981. "Approximate riemann solvers, parameter vectors, and difference schemes". *Journal of Computational Physics*, Vol. 43, No. 2, pp. 357–372. ISSN 0021-9991. doi:https://doi.org/10.1016/0021-9991(81)90128-5. URL https://www.sciencedirect.com/science/article/pii/0021999181901285.

Rusanov, V., 1961. "Calculation of interaction of non-steady shock waves with obstacles". *jour Zh. Vychisl. Mat. Mat. Fiz.*, Vol. 1, No. 2, pp. 267–279.

Starzmann, J., Hughes, F.R., Schuster, S., White, A.J., Halama, J., Hric, V., Kolovratník, M., Lee, H., Sova, L., Šťastný, M., Grübel, M., Schatz, M., Vogt, D.M., Patel, Y., Patel, G., Turunen-Saaresti, T., Gribin, V., Tishchenko, V., Gavrilov, I., Kim, C., Baek, J., Wu, X., Yang, J., Dykas, S., Wróblewski, W., Yamamoto, S., Feng, Z. and Li, L., 2018. "Results of the international wet steam modeling project". *Proceedings of the Institution of Mechanical Engineers, Part A: Journal of Power and Energy*, Vol. 232, No. 5, pp. 550–570. doi:10.1177/0957650918758779. URL https://doi.org/10.1177/0957650918758779.

Vitale, S., Gori, G., Pini, M., Guardone, A., Economon, T., Palacios, F., Alonso, J. and Colonna, P., 2015. "Extension of the SU2 open source CFD code to the simulation of turbulent flows of fluids modelled with complex thermophysical laws". In *22nd AIAA Computational Fluid Dynamics Conference*. doi:10.2514/6.2015-2760. URL https://arc.aiaa.org/doi/abs/10.2514/6.2015-2760.

7. RESPONSIBILITY NOTICE

The authors are solely responsible for the printed material included in this paper.